ELSEVIER

New Astronomy 7 (2002) 553–575

New Astronomy

www.elsevier.com/locate/newast

Morphological analysis of open clusters' properties II. Relationships projected onto the galactic plane

A.L. Tadross[a,*], P. Werner[b], A. Osman[a], M. Marie[c]

[a] *National Research Institute of Astronomy and Geophysics, 11421-Helwan, Cairo, Egypt*
[b] *Astrophys. Inst. and Univ. Obs. (AIU), Schillergaesschen 2–3, D-07745 Jena, Germany*
[c] *Faculty of Science, Astronomy Department, Cairo University, Cairo, Egypt*

Received 26 June 2001; received in revised form 1 July 2002; accepted 1 August 2002
Communicated by G.F. Gilmore

Abstract

A morphological analysis study of open clusters' properties has been achieved for a sample of 160 UBVCCD open star clusters of approximately 128,000 stars near the galactic plane. The data was obtained and reduced from Tadross (2001) using the same reduction procedures, which makes this catalogue the largest homogeneous source of open clusters' parameters.

PACS: 98.20.d; 98.20.Di; 98.35.Hj; 98.00.00
Keywords: Galaxy: open clusters and associations: general; Galaxy: structure; Galaxy: disk; Galaxy: formation

1. Introduction

Open star clusters are more effective than field stars in solving problems of star formation and stellar evolution that improve our knowledge about the distance scale and the kinematic characteristics of the Milky Way. This kind of study requires large sets of homogeneous data on the positions and ages of the galactic objects. The most suitable objects for these studies are open clusters because of the precision in estimating their ages; reddenings and distances, which can be determined with good precision from their color magnitude diagrams. In galactic astronomy open clusters play a central role in virtually every problem (Majewski et al., 2001). In the future, the galactic distance scale will be studied with higher accuracy, clusters' ages and stellar evolution can be studied using the Space Interferometry Mission (SIM) that are able to obtain about 2% parallax distances approximately to the galactic center (Worthey, 2001). Also, GAIA satellite will provide more precision measurements that need to produce a stereoscopic and kinematics census of about one billion stars throughout our Galaxy, amounting to about 1 percent of the galactic stellar population.

*Corresponding author. Tel.: +20-2-5560-645; fax: +20-2-5548-020.
E-mail addresses: altadross@mailer.scu.eun.eg (A.L. Tadross), altadross@yahoo.com (A.L. Tadross), pfau@astro.uni-jena.de (P. Werner), amiosman@mailer.scu.eun.eg (A. Osman), mohmarie@mailer.scu.eun.eg (M. Marie).

1384-1076/02/$ – see front matter
PII: S1384-1076(02)00172-0

GAIA's main scientific goal is to clarify the origin and history of our Galaxy (Perryman et al., 2001). Before those space missions, it is useful for this kind of study to reinvestigate the properties of the galactic structure, using the most recent UBVCCD observations for a large sample of open clusters as homogeneously analyzed in Tadross (2001).

2. On the comparison of the clusters' parameters

Although the catalog of Lyngå (1987, 5th edition) is the most famous catalog of the known open clusters' parameters, it has not been updated since that date and now is partly obsolete because many new clusters have been observed in the last decade. In this respect, the known web page of the 'Database of Open Clusters' by J.C. Mermilliod tries to keep Lyngå catalog updated. Regarding the modern catalogs, we found that Loktin and Matkin have published the first version of their catalog in 1994. It contained information for 320 clusters in the UBV system. In 1997, Malysheva published a catalog of parameters for 73 open clusters determined from the uvbyβ photometry; his values are in good agreement with those of Loktin and Matkin (1994). The improved version catalog of Loktin et al. has been published in 1997; it contained the updated parameters of homogeneously estimated reddenings, distances, and ages for 367 open clusters. Dambis (1999) determined the same parameters for 203 open clusters based on the published photoelectric and CCD data, using the ZAMS of Kholopov (1980a,b) and the evolutionary deviation curves of Maeder and Meynet (1991). Dutra and Bica (2000) have studied 103 galactic open clusters and compared the reddening values obtained from far infrared IRAS and COBE observations with those obtained from visible observations. In addition, there is some recent literature for further determination of cluster parameters obtained from new BV, BVI or VI CCD observations. The main problem with those recent data is the difficulty of estimating the amount of reddening, because of the absence of U band. Therefore, reddening is estimated, either by comparison with clusters presenting a similar color-magnitude diagram, or by direct adjustment of a theoretical isochrone of an appropriate metallicity.

On the comparison of our parameters (reddening, distances and ages) with the others, it is important to declare that the parameters in Tadross (2001) have been re-investigated here except for the metallicity that will be presented in a separate study, see Table 1. So, our parameters have been compared with the most recent catalogs that have UBV photometric data, namely, they have been compared with Lyngå (1987), Loktin and Matkin (1994), Loktin et al. (1997), Friel (1995), Twarog et al. (1997) and Dambis (1999) as shown in Fig. 1A and 1B. The number of shared clusters between them and us, and the correlation coefficients have been presented in Table 2.

Table 1 contains the clusters' parameters in which this study is based on. Column 1 gives the cluster designation, columns 2–5: the clusters' coordinates for equinox 2000.00. Column 6: reddening values, where asterisks denote the clusters with variable reddening, column 7: the mean distance modulus. Column 8: the distance from the Sun after the correction of absorption, column 9: the age in logarithmic form. Column 10: the clusters' linear diameters. Columns 11–12: the galactic rectangular coordinates X and Y from the Sun on the galactic plane, column 13: the cluster height Z from the galactic plane. Column 14: the clusters' distances from the galactic center, column 15: the visual luminosity, column 16: the clusters' member richness, column 17: the mass of the cluster.

3. Parameters' relations

The distribution of our sample according to the distances from the galactic center, Rgc, and the height from the galactic plane, Z, is presented in Fig. 2; the arrow refers to the cluster Be 29 that has the maximum distance from the galactic center. Therefore, we can see that the clusters with $Rgc < 10.5$ kpc and $ages < Hyades$ ($7*10^8$ yr) are strongly concentrated to the galactic plane. While at large distances, $Rgc > 10.5$ kpc, the clusters become more dispersed from the galactic plane and older than Hyades (cf. Friel, 1995). However, the relations between clusters' properties like age, diameter,

Table 1
Clusters' parameters

Cluster	R.A. (h. min.)	Dec. (° ′)	G. Long.	G. Lat.	E_{B-V}	$\langle V-M_v\rangle$	Dist.	Log t	Diam.	G.X.	G.Y.	Z.	Rgc	M_v	Mem.	Mass
NGC 103	00 25.2	61 20	119.80	−1.38	0.48*	14.10	3221	7.70	4.44	2.79	1.60	−77.57	10.48	−5.33	1596	2100
NGC 129	00 29.9	60 13	120.25	−2.54	0.54	12.80	1622	7.80	9.91	1.40	0.82	−71.92	9.42	−4.92	538	800
NGC 146	00 33.1	63 17	120.87	0.49	0.52	13.30	2100	7.40	3.66	1.80	1.08	159.67	9.75	−6.47	222	727
NGC 188	00 44.4	85 20	122.78	22.46	0.05	11.10	1540	9.70	6.13	1.20	0.77	588.31	9.36	−1.31	211	208
NGC 366	01 06.5	62 14	124.68	−0.59	1.18*	15.90	2588	7.34	2.82	2.13	1.47	−26.65	10.20	−4.72	597	713
NGC 381	01 08.3	61 35	124.94	−1.22	0.36	11.30	1062	9.00	1.93	0.87	−0.61	−22.61	9.15	−2.42	505	492
NGC 433	01 15.3	60 08	125.90	−2.60	0.56*	14.10	2858	7.60	2.62	2.31	1.67	−129.65	10.43	−5.57	1056	1415
NGC 436	01 15.7	58 49	126.07	−3.91	0.47*	14.00	3122	7.80	5.02	2.52	1.83	−212.92	10.64	−4.58	443	653
NGC 457	01 19.1	58 20	126.56	−4.35	0.50	13.90	2851	7.35	9.83	2.28	−1.69	−216.24	10.45	−6.44	1608	2399
NGC 581	01 33.2	60 43	128.02	−1.76	0.46	13.75	2825	7.10	5.51	2.22	−1.74	−86.76	10.48	−7.40	1550	2303
NGC 637	01 43.0	64 00	128.55	1.70	0.45	12.90	1939	7.22	2.00	1.52	1.21	57.51	9.83	−4.52	55	103
NGC 654	01 44.1	61 53	129.09	−0.35	0.90	14.90	2483	7.42	3.70	1.93	−1.56	−15.17	10.25	−6.20	323	763
NGC 663	01 46.1	61 15	129.46	−0.94	0.75*	14.40	2469	7.30	11.72	1.91	1.57	−40.50	10.25	−6.31	1643	2365
NGC 869	02 19.1	57 09	134.63	−3.72	0.58	14.20	2904	7.10	24.67	2.06	2.04	−188.41	10.74	−8.63	240	1146
NGC 884	02 22.5	57 07	135.08	−3.60	0.50	13.60	2483	7.20	19.39	1.75	1.75	−155.91	10.40	−7.26	95	471
NGC 1039	02 42.0	42 47	143.64	−15.60	0.05	8.40	444	8.70	4.64	0.25	0.34	−119.43	8.85	−1.58	175	190
NGC 1193	03 05.8	44 22	146.81	−12.18	0.21*	14.60	6074	9.30	3.66	3.25	4.97	−1281.59	13.91	−3.17	380	480
NGC 1245	03 14.7	47 15	146.64	−8.93	0.27*	12.60	2211	9.16	6.51	1.20	1.82	−343.14	10.40	−3.19	358	434
NGC 1750	05 03.9	23 39	179.18	−10.70	0.33	10.20	669	8.40	?	0.01	0.66	−124.21	9.16	−4.07	761	823
NGC 1798	05 11.9	47 37	160.76	4.85	0.50	14.80	4315	9.15	6.28	1.42	4.06	364.84	12.64	−5	580	796
NGC 1907	05 28.0	35 19	172.62	0.31	0.43	12.40	1587	8.60	2.73	0.20	1.57	8.58	10.08	−4.25	157	257
NGC 1931	05 31.4	34 15	173.90	0.28	0.66*	14.00	2350	7.45	1.07	0.25	2.34	11.48	10.84	−4.38	78	160
NGC 2112	05 53.9	00 24	205.90	−12.61	0.60	11.50	813	9.45	2.64	−0.35	0.71	−177.45	9.22	−1.99	261	283
NGC 2158	06 07.4	24 05	186.64	1.76	0.40	14.80	5012	9.20	7.67	−0.58	4.97	153.93	13.49	−2.02	200	242
NGC 2168	06 08.8	24 20	186.58	2.18	0.24	10.45	859	8.00	7.12	−0.09	0.85	32.68	9.35	−4.85	453	766
NGC 2192	06 15.2	39 51	173.41	10.64	0.22	13.35	3365	9.00	5.77	0.38	3.29	621.31	11.81	−3.45	153	282
NGC 2204	06 15.7	−18 38	226.01	−16.07	0.08	13.60	4656	9.20	16.03	−3.22	3.11	−1288.8	12.11	−4.57	1030	1209
NGC 2243	06 29.8	−31 16	239.50	−17.97	0.00	13.00	3981	9.40	5.78	−3.26	1.92	−1228.28	10.99	−2.57	505	544
NGC 2244	06 32.4	04 52	206.42	−2.02	0.44*	12.70	1795	6.80	12.04	0.80	1.61	−63.27	10.14	−7.7	323	1064
NGC 2264	06 41.0	09 53	202.94	2.2	0.10	08.30	0394	7.51	2.29	−0.15	−0.36	15.12	8.86	−2.76	359	330
NGC 2266	06 43.2	26 58	187.78	10.28	0.10	13.20	3758	8.90	6.33	−0.50	3.66	670.72	12.19	−3.87	309	417
NGC 2355	07 16.9	13 46	203.36	11.80	0.112	11.775	1915	8.98	5.13	−0.74	1.72	391.64	10.26	−2.88	179	232
NGC 2383	07 24.7	−20 55	235.26	−2.44	0.28	13.33	3048	7.60	5.07	−2.50	1.74	−129.76	10.54	−3.89	358	524
NGC 2384	07 25.0	−21 01	235.39	−2.41	0.28	13.00	2618	7.00	2.40	−2.15	1.49	−110.09	10.22	−5.7	199	327
NGC 2420	07 38.5	21 34	198.11	19.65	0.00	12.19	2742	9.30	7.55	−0.80	2.45	921.92	11.02	−3.45	451	524
NGC 2421	07 36.3	−20 36	236.24	0.08	0.48	13.39	2317	7.70	7.09	−1.93	1.29	3.24	9.98	−4.27	83	130
NGC 2439	07 40.8	−31 38	246.42	−4.42	0.37	14.025	3669	7.59	10.95	−3.35	1.46	−282.73	10.52	−5.81	72	190
NGC 2453	07 47.8	−27 13	243.33	−0.94	0.40	13.90	3311	7.00	4.94	−2.96	1.49	−54.32	10.42	−4.33	147	327
NGC 2477	07 52.3	−38 32	253.58	−5.83	0.28	11.60	1374	9.00	11.04	−1.31	−0.39	−139.57	8.98	−5.30	1730	2073
NGC 2489	07 56.2	−30 03	246.71	−0.78	0.40*	11.60	1148	8.25	2.73	−1.05	0.45	−15.63	9.02	−2.53	64	100
NGC 2506	08 00.2	−10 47	230.57	9.91	0.01	12.90	3745	9.10	6.67	−2.85	2.34	644.59	11.23	−3.78	691	879
NGC 2516	07 58.4	−60 51	273.94	−15.88	0.10	08.40	412	7.80	3.47	−0.39	−0.03	−112.73	8.48	0.85	33	36
NGC 2567	08 18.6	−30 38	249.81	2.98	0.15	11.55	1631	8.60	4.18	−1.53	0.56	84.80	9.19	−3.81	93	125
NGC 2627	08 37.3	−29 56	251.58	6.65	0.05	11.065	1515	8.60	3.94	−1.43	0.47	175.48	9.09	−1.60	72	81
NGC 2658	08 43.4	−32 38	254.56	6.07	0.40	14.10	3631	8.37	12.93	−3.48	0.96	383.93	10.09	−3.91	94	155
NGC 2660	08 42.3	−47 08	265.86	−3.03	0.40	13.50	2754	9.10	3.32	−2.74	0.20	−145.59	9.12	−4.1	695	827
NGC 2670	08 45.5	−48 46	267.47	−3.61	0.43	12.10	1382	8.00	3.57	−1.38	0.06	−87.02	8.67	−2.01	150	185
NGC 2682	08 51.4	11 49	215.58	31.72	0.04	9.630	794	9.60	6.39	−0.39	0.55	417.63	9.07	−3.43	933	820
NGC 2818	09 16.0	−36 35	261.98	8.59	0.20	13.00	2951	8.90	7.68	−2.89	0.41	440.80	9.37	−3.49	214	288
NGC 2910	09 30.4	−52 53	275.29	−1.18	0.11	11.10	1408	8.10	2.68	−1.40	−0.13	−28.99	8.49	−2.09	44	62
NGC 3114	10 02.7	−60 06	283.34	−3.83	0.00	9.80	912	8.20	9.29	−0.88	−0.21	−60.92	8.34	−1.85	104	130

Table 1. Continued

Cluster	R.A. (h. min.)	Dec. (° ′)	G. Long.	G. Lat.	E_{B-V}	$\langle V-M_v\rangle$	Dist.	Log t	Diam.	G.X.	G.Y.	Z.	Rgc	M_v	Mem.	Mass
NGC 3603	11 15.0	−61 14	291.62	−0.52	1.40	17.40	3715	6.80	2.70	−3.45	−1.37	−32.70	7.92	−7.05	56	427
NGC 3766	11 36.1	−61 35	294.11	−0.03	0.20	12.40	2239	7.40	7.33	−2.04	−0.91	−1.17	7.85	−7.18	1640	2780
NGC 4103	12 06.7	−61 13	297.57	1.17	0.30	12.15	1718	7.50	3.16	−1.52	−0.79	35.08	7.85	−4.13	117	211
NGC 4755	12 53.6	−60 16	303.21	2.53	0.382	12.54	1818	7.53	5.43	−1.52	−0.99	80.27	7.66	−5.17	364	682
NGC 4815	12 58.1	−64 56	303.63	−2.09	0.78	14.775	2805	8.38	2.69	−2.33	−1.55	−102.31	7.33	−5.89	1431	2478
NGC 5168	13 31.2	−60 56	307.74	1.57	0.84	15.00	2844	8.34	3.81	−2.25	−1.74	77.93	7.12	−4.34	147	353
NGC 5460	14 07.6	−48 18	315.78	12.65	0.14	9.30	588	8.40	3.94	−0.40	−0.41	126.66	8.10	−2.04	45	58
NGC 5606	14 27.8	−59 38	314.84	0.99	0.50	13.00	1884	7.00	2.09	−1.33	−1.33	32.55	7.30	−5.46	103	251
NGC 5617	14 29.7	−60 42	314.67	−0.10	0.491	13.04	1945	7.90	5.48	−1.38	−1.37	−3.39	7.27	−3.93	112	230
NGC 5662	14 35.2	−56 32	316.90	3.47	0.32	10.20	679	8.00	2.34	−0.46	−0.49	41.11	8.02	−2.29	147	142
NGC 6005	15 55.9	−57 24	325.79	−2.99	0.56	13.60	2270	8.90	2.47	−1.87	1.27	−118.40	9.95	−3.94	326	483
NGC 6067	16 13.2	−54 11	329.76	−2.20	0.36	12.40	1762	7.93	6.77	−0.89	−1.52	−67.64	7.04	−5.23	627	974
NGC 6087	16 18.9	−57 53	327.76	−5.40	0.20	10.30	851	8.00	2.93	−0.45	−0.72	−80.10	7.79	−2.08	370	288
NGC 6134	16 27.8	−49 08	334.92	−0.19	0.44	11.25	920	9.05	1.95	−0.39	−0.83	−3.05	7.68	−1.73	61	82
NGC 6192	16 40.4	−43 21	340.65	2.12	0.67	13.35	1716	8.00	3.74	−0.57	−1.62	63.48	6.91	−4.69	81	244
NGC 6204	16 46.5	−47 01	338.59	−1.08	0.46	11.85	1178	7.86	2.03	−0.43	−1.10	−22.20	7.42	−3.39	124	200
NGC 6231	16 54.0	−41 47	343.47	1.22	0.48*	12.65	1652	6.50	6.32	−0.47	1.58	35.17	6.93	−7.7	391	1470
NGC 6253	16 59.0	−52 42	335.46	−6.25	0.20	11.55	1514	9.70	2.43	−0.62	−1.37	−164.78	7.16	−2.61	807	683
NGC 6451	17 50.7	−30 12	359.48	−1.61	0.70	13.70	1928	8.22	4.35	−0.02	−1.93	−54.16	6.57	−4.41	153	339
NGC 6475	17 53.9	−34 47	355.86	−4.53	0.04	7.18	257	8.55	5.76	−0.02	−0.26	−20.30	8.24	−1.03	125	127
NGC 6520	18 03.3	−27 53	2.88	−2.86	0.44	12.45	1600	8.34	3.18	0.08	−1.59	−79.81	6.91	−4.06	163	250
NGC 6603	18 18.5	−18 24	12.86	−1.32	0.56*	12.80	1570	8.80	1.86	0.35	−1.53	−36.17	6.98	−3.62	509	584
NGC 6611	18 18.8	−13 45	16.99	0.79	0.68*	13.30	1652	6.50	3.60	0.48	−1.58	125.6	6.94	−3.45	282	435
NGC 6633	18 27.7	06 4	36.09	8.28	0.15	8.20	348	8.70	2.77	0.20	−0.28	50.12	8.22	0.53	53	53
NGC 6649	18 33.4	−10 23	21.64	−0.78	1.30*	14.95	1396	8.00	2.19	0.51	−1.30	−19.01	7.22	−5.65	320	740
NGC 6705	18 51.1	−06 16	27.31	−2.77	0.45	12.94	1975	8.26	5.44	0.90	−1.75	−95.43	6.81	−5.74	369	936
NGC 6709	18 51.5	10 20	42.16	4.70	0.28	11.40	1253	8.00	4.51	0.84	−0.93	102.68	7.62	−4.04	328	458
NGC 6716	18 54.6	−19 52	15.39	−9.59	0.10	09.45	0670	8.25	1.73	0.17	0.64	−111.62	7.87	−3.12	259	343
NGC 6755	19 07.8	04 14	38.55	−1.70	0.78*	14.05	2009	8.16	7.73	1.25	−1.57	−59.60	7.04	−3.26	80	160
NGC 6791	19 20.8	37 51	70.01	10.96	0.22	13.40	3548	10.00	13.30	3.27	−1.19	674.58	8.04	−3.61	1278	1214
NGC 6823	19 43.2	23 18	59.41	−0.15	0.82*	13.65	1574	6.82	5.42	1.35	−0.80	−4.12	7.82	−5.16	23	116
NGC 6871	20 05.9	35 46	72.64	2.08	0.45*	12.80	1851	7.00	10.98	1.76	0.55	67.20	8.14	−7.92	622	1689
NGC 6913	20 23.9	38 32	76.92	0.60	0.55*	12.20	1209	7.20	2.36	1.18	−0.27	12.66	8.31	−4.14	90	222
NGC 7044	21 13.0	42 29	85.87	−4.13	0.57	14.20	2948	9.20	6.41	2.93	−0.21	−212.30	8.80	−3.5	905	1025
NGC 7128	21 44.0	53 43	97.35	0.42	0.99*	15.20	2492	7.20	2.57	2.47	0.32	18.26	9.16	−5.09	17	110
NGC 7142	21 45.9	65 48	105.42	9.45	0.21	11.35	1360	9.70	3.54	1.29	0.36	223.27	8.95	−1.67	292	295
NGC 7235	22 12.6	57 17	102.72	0.78	0.95*	15.40	2901	7.00	3.99	2.83	0.64	39.49	9.57	−7.84	197	1169
NGC 7245	22 15.3	54 20	101.37	−1.87	0.55	13.50	2200	8.60	3.16	2.16	0.43	−71.80	9.19	−3.21	37	80
NGC 7380	22 47.0	58 06	107.08	−0.90	0.50	12.40	1429	7.00	4.99	1.36	0.42	−22.44	9.02	−5.93	344	731
NGC 7419	22 54.3	60 50	109.13	1.14	1.56*	15.70	1337	7.20	1.64	1.26	0.44	101.65	9.03	−4.65	246	456
NGC 7510	23 11.5	60 34	110.96	0.05	1.00*	15.19	2443	7.78	2.81	2.28	0.87	2.13	9.65	−5.96	256	655
NGC 7762	23 49.9	68 01	117.20	5.84	0.99	13.30	1040	8.89	3.34	0.92	0.47	105.79	9.02	−2.90	84	137
NGC 7789	23 57.0	56 43	115.49	−5.36	0.26	12.30	1954	9.18	7.92	1.75	0.84	−182.56	9.50	−4.53	791	915
NGC 7790	23 58.4	61 12	116.59	−1.01	0.62	14.95	3864	7.98	8.87	3.45	1.73	−68.10	10.80	−5.35	248	565
IC 348	03 44.6	32 18	160.43	−17.74	0.62	9.40	300	7.30	0.57	0.09	0.27	−91.41	8.77	−1.76	118	71
IC 1311	20 10.4	41 13	77.70	4.25	0.30	14.75	5689	9.30	13.06	5.54	−1.21	421.57	9.17	−3.91	517	670
IC 1590	00 53.1	56 35	123.16	−6.29	0.31	13.35	2941	6.50	?	2.45	1.60	−322.22	10.40	−4.47	77	189
IC 1805	02 32.7	61 27	134.74	0.92	0.80*	14.30	2188	6.70	13.18	1.55	1.54	35.13	10.16	−8.25	226	1191
IC 2602	10 43.2	−64 23	289.60	−4.90	0.04	5.70	136	7.50	2.13	−0.13	−0.04	−11.63	8.46	0.65	79	74
IC 4651	17 24.7	−49 55	340.07	−7.88	0.02	9.50	771	9.34	2.65	−0.26	−0.72	−105.69	7.79	−1.0	107	100
IC 4665	17 46.2	05 43	30.61	17.08	0.16	8.10	333	7.60	4.37	0.16	−0.27	97.82	8.23	−3.39	169	222
IC 4996	20 16.4	37 39	75.36	1.31	0.66	13.40	1782	7.20	2.59	1.72	−0.45	40.75	8.23	−6.37	318	529

Table 1. Continued

Cluster	R.A. (h. min.)	Dec. (° ′)	G. Long.	G. Lat.	E_{B-V}	$\langle V-M_v\rangle$	Dist.	Log t	Diam.	G.X.	G.Y.	Z.	Rgc	M_v	Mem.	Mass
Am 2	07 39.7	−33 27	247.88	−5.51	0.59	16.70	9047	9.70	66.66	−8.34	3.39	−868.68	14.55	−4.10	357	413
Be 1	00 09.7	60 25	117.79	−2.03	0.32	11.00	0982	7.60	1.37	0.87	−0.46	−34.79	9.00	−1.29	64	84
Be 2	00 25.2	60 23	119.70	−2.31	0.80*	15.90	4571	8.90	5.25	3.97	2.26	−184.24	11.74	−3.96	122	219
Be 7	01 54.2	62 22	130.13	0.37	0.80*	14.40	2291	6.70	2.63	1.75	1.48	14.79	10.13	−4.65	411	584
Be 14	05 00.2	43 28	162.86	0.71	0.53*	15.35	5395	9.20	13.42	1.59	5.15	66.85	13.75	−6.6	1243	1826
Be 17	05 20.6	30 36	175.65	−3.65	0.60	14.00	2570	9.90	9.29	0.19	2.56	−163.63	11.06	−2.29	413	393
Be 21	05 51.7	21 47	186.83	−2.5	0.60*	14.50	3236	7.80	5.95	−0.38	−3.21	−141.15	11.72	−4.4	306	402
Be 22	05 58.4	07 50	199.80	−8.05	0.62	16.00	6266	9.48	3.83	−2.10	5.84	−877.49	14.52	−3.29	620	727
Be 28	06 49.5	03 00	210.39	1.52	0.78	15.475	3873	8.10	5.63	−1.96	3.34	98.37	12.00	−3.97	52	146
Be 29	06 53.1	16 55	197.98	8.03	0.21	17.30	21062	9.04	18.13	−6.44	19.84	534.97	29.26	−4.56	578	869
Be 30	06 55.1	03 17	210.80	2.89	0.51	15.00	4661	8.50	?	−2.38	−3.99	118.39	12.73	−5.18	595	888
Be 31	06 54.9	08 20	206.26	5.12	0.13	14.80	7508	9.38	11.36	−3.31	6.71	190.70	15.59	−2.90	353	427
Be 32	06 57.4	06 30	207.95	4.40	0.15	13.455	3922	9.40	7.70	−1.83	3.45	99.62	12.1	−3.64	620	698
Be 33	06 57.8	−13 13	225.43	−4.62	0.62	15.60	5212	8.68	8.72	−5.03	1.31	132.38	11.03	−5.88	1128	1619
Be 39	07 46.7	−04 35	223.47	10.09	0.13	13.50	4126	9.90	13.02	−2.79	2.95	722.80	11.81	−3.66	1548	1476
Be 42	19 05.1	01 52	36.17	−2.19	0.66	11.92	902	9.80	1.31	0.53	−0.73	−34.45	7.80	0.64	135	87
Be 58	00 00.2	60 58	116.75	−1.29	0.54	13.45	2188	8.20	4.40	1.95	−0.98	−49.25	9.68	−4.31	184	358
Be 60	00 17.7	60 57	118.85	−1.64	0.37	12.80	2089	8.20	2.52	1.83	−1.01	−59.795	9.68	−1.49	101	134
Be 62	01 01.1	63 57	123.99	1.1	0.77	14.40	2396	7.60	7.11	1.99	−1.34	45.99	10.04	−5.39	731	990
Be 64	02 21.0	65 53	131.92	4.60	1.06	16.15	3475	9.00	3.60	2.58	2.31	278.69	11.12	−2.29	32	58
Be 69	05 24.6	32 38	174.42	−1.79	0.75	14.85	3475	8.90	3.99	0.34	3.46	−108.56	11.96	−3.18	107	177
Be 79	18 45.2	−01 12	31.14	0.84	0.99*	14.10	1764	8.30	4.67	0.91	−1.51	25.86	7.05	−1.36	31	67
Be 81	19 01.5	−00 31	33.64	−2.51	1.00	14.80	2042	9.00	4.16	1.13	−1.70	−89.43	6.89	−4.06	886	1038
Be 86	20 20.4	38 42	76.66	1.26	0.70*	12.60	1161	7.00	2.33	1.13	−0.28	25.54	8.31	−6.52	220	733
Be 93	21 56.2	63 57	105.07	7.32	1.50	18.80	6095	8.00	7.09	5.84	1.57	776.62	11.67	−4.08	641	150
Be 99	23 21.6	71 45	115.95	10.11	0.30	14.40	4842	9.50	8.06	4.29	2.08	849.96	11.45	−2.53	422	447
Bo 2	06 48.8	00 23	212.30	−0.40	0.81*	16.50	5936	6.88	3.63	−3.17	5.02	−41.44	13.88	−7.35	29	219
Coll 74	05 48.5	07 24	198.98	−10.40	0.38	13.00	2254	9.20	2.56	−0.72	2.10	−406.89	10.63	−2.68	278	310
Coll 261	12 37.7	−68 28	301.69	−5.64	0.26	12.60	2244	9.95	?	−1.90	−1.17	56.99	7.57	−2.62	1286	1127
Coll 272	13 30.6	−61 16	307.62	1.25	0.44	13.20	2259	7.20	6.48	−1.79	−1.38	49.29	7.34	−5.35	702	1013
Doli 25	06 45.0	00 18	211.94	−1.29	0.80	16.10	5012	7.10	33.53	−2.65	4.25	−112.83	13.03	−5.65	64	249
Ki 2	00 51.1	58 11	122.88	−4.67	0.38	15.20	6209	9.80	8.07	5.20	3.36	−505.49	12.96	−2.68	471	491
Ki 7	03 59.0	51 48	149.76	−1.04	1.25	16.00	2440	8.60	3.50	1.23	2.11	−44.29	10.68	−4.97	342	633
Ki 10	22 55.0	59 10	108.49	−0.40	1.16*	16.55	3597	7.70	4.41	3.41	1.14	−25.12	10.23	−5.65	161	527
Ki 11	23 47.8	68 37	117.16	6.47	1.02	14.975	2148	9.70	2.46	1.90	0.97	242.02	9.67	−2.16	361	384
Ki 15	00 33.0	61 51	120.75	−0.95	0.46	13.70	2761	8.60	2.01	2.37	1.41	−45.77	10.19	−3.69	1082	1164
Ru 32	07 45.0	−25 30	241.54	−0.60	0.34	13.30	4159	7.78	7.00	−3.66	1.98	−43.55	11.10	−3.30	80	130
Ru 79	09 41.0	−53 48	277.09	−0.80	0.78	14.70	2710	7.65	8.67	−2.69	−0.33	−37.84	8.59	−5.01	129	340
Tr 1	01 35.6	61 18	128.22	−1.14	0.60*	14.00	2570	7.40	2.95	2.02	1.59	−51.13	10.29	−5.17	315	548
Tr 5	06 36.7	09 27	202.86	1.05	0.58	14.24	2958	9.10	6.50	−1.15	2.72	54.21	11.28	−5.75	3759	4313
Tr 11	10 04.9	−61 36	284.46	−4.85	0.20	13.00	2951	8.26	4.29	−2.85	−0.73	−249.52	8.28	−3.78	163	246
Tr 14	10 43.9	−59 33	287.42	−0.58	0.50	13.55	2427	7.10	3.71	−2.31	−0.73	−24.56	8.11	−6.51	77	442
Haf 6	07 20.1	−13 07	227.85	0.25	0.43	13.90	3166	9.00	4.12	−2.35	2.12	13.81	10.88	−3.39	482	571
Haf 18	07 52.5	−26 21	243.11	0.44	0.70	16.50	6998	7.00	3.22	−6.24	3.16	53.74	13.23	−5.1	17	96
Haf 19	07 52.7	−26 14	243.04	0.52	0.46	15.70	6934	7.35	3.97	−6.18	3.14	62.93	13.18	−2.74	22	57
Ly 6	16 04.8	−51 54	330.37	0.34	1.34	16.00	2133	7.60	3.10	−1.05	−1.85	12.66	6.73	−4.96	53	181
Melo 20	03 22.1	48 37	146.95	−7.11	0.02	6.30	177	7.80	9.45	0.09	0.15	−21.86	8.65	−1.13	96	106
Melo 105	11 19.4	−63 29	292.89	−2.45	0.52	13.30	2099	8.30	2.41	−1.93	−0.81	−89.73	7.92	−4.21	107	228
Pis 3	08 30.9	−38 39	257.86	0.46	1.33	14.80	1246	9.28	2.48	−1.22	0.26	10.00	8.85	−3.24	548	635
Pis 18	13 36.6	−62 09	308.18	0.26	0.50	13.20	2065	9.00	2.73	−1.62	−1.28	9.37	7.40	−3.1	240	323
Pis 20	15 15.5	−59 03	320.52	−1.21	1.14	15.80	2624	6.70	1.50	−1.67	−2.02	−55.42	6.68	−4.59	83	254

Table 1. Continued

Cluster	R.A. (h. min.)	Dec. (° ′)	G. Long.	G. Lat.	E_{B-V}	$\langle V-M_v\rangle$	Dist.	Log t	Diam.	G.X.	G.Y.	Z.	Rgc	M_v	Mem.	Mass
To 2	07 03.9	−20 51	232.95	−6.73	0.37*	16.00	9110	9.08	8.69	−7.22	5.45	−1067.56	15.74	−5.73	2041	2951
Sh 1	11 00.1	−60 21	289.58	−0.42	1.35	18.80	7630	6.95	1.33	−7.19	−2.56	580.10	9.33	−5.92	10	96
Stock 24	00 39.7	61 57	121.55	−0.88	0.50	13.80	2723	8.00	3.13	2.32	1.42	−41.82	10.19	−4.79	948	1155
Wes 2	10 23.9	−57 44	284.26	−0.33	1.60	18.80	5248	7.59	2.01	−5.09	−1.30	−30.23	8.82	−7.91	58	513
Eso 18	10 15.9	−64 37	287.22	−6.59	0.26	15.70	9354	9.70	9.25	−8.87	2.75	−1073.51	10.63	−4.15	865	1043
Eso 96	13 18.1	−65 55	305.35	−3.17	0.75	17.70	11285	8.90	?	−9.19	−6.52	−623.03	9.41	−5.22	580	984

height on the galactic plane, and so on, are presented in the following sections.

3.1. Reddening and distance estimation

Reddening estimation is the first step in the cluster compilation. It affects the distance determination via the main sequence fitting, and consequently affected all the cluster's dimensions and positions in the Galaxy. Increasing reddening correction moves the main sequence toward the blue, where reddening degree is depending upon the color of the star; a change in the intrinsic color $(B-V)_o$ of 1 mag lowers the effective reddening $E(B-V)$ by approximately 10% (Fernie, 1963). Thus, corrections to the distance modulus for increased reddening make the true modulus smaller. However, the exact impact on the distance estimate of changing the reddening is unique to each photometric system (Twarog et al., 1997). Main sequence fitting was applied to the most clusters sample, changing $E(B-V)$ alters the true modulus by $A_v = 3.25 * E(B-V)$; for more details see Tadross (2001).

3.2. Reddening distribution

The distribution of the reddening of our sample versus the galactic latitudes confirms that the higher values of reddening are concentrated on and near the galactic plane as shown in Fig. 3A. Along the galactic longitude bins of 20 degrees the distribution of the mean reddening at each bin show that the higher values are concentrated around longitude of 130 near the feature region of Perseus arm, the external youngest arm of the Galaxy, see Fig. 3B. The clusters' numbers from which the mean reddening have been calculated and the standard deviation of each bin are tabulated in Table 3.

Fig. 4 shows a contour map of the reddening distribution from the Sun on the galactic plane, the higher values are found to be concentrated at particular feature patterns. Dividing the reddening to three ranges: $E_{B-V} < 0.50$, $0.50 < E_{B-V} < 1.00$ and $E_{B-V} > 1.00$ mag., we found that 16%, 41% and 53% clusters, respectively, are defined as clusters with variable reddening. The difference between the maximum and minimum reddening of those clusters are found to be more than (0.11 mag.) the natural dispersion criterion as described by Burki's (1975). The distribution of such clusters on the galactic plane shows that they exist in higher extinction regions of the local spiral arms: Perseus, Carina and Sagittarius. The positions of these features on the galactic plane have the approximate coordinates:

	G.X. kpc	*G.Y. kpc*
Perseus	1.5	1.5
Carina	−2.2	−1.0
Sagittarius	0.0	−1.4

As shown in Fig. 5, the general trend of the reddening with ages shows that the reddening towards the clusters decreases with age: younger clusters, which are located in the spiral arms of the Galaxy, tend to be more reddened than older ones.

3.3. Diameter–galactic height and galactocentric distance

Linear diameters of our sample have been plotted versus the absolute values of the height ($|Z|$) on the galactic plane in three ranges of galactocentric radii: $Rgc < 8$, $8 < Rgc < 9.5$ and $Rgc > 9.5$ kpc, as shown in Fig. 6, and in three age intervals: $t < 10^{8.0}$, $10^{8.0} < t < 10^{9.5}$, and $t > 10^{9.5}$ yr, as shown in Fig. 7. The solar vicinity is chosen to lie between the

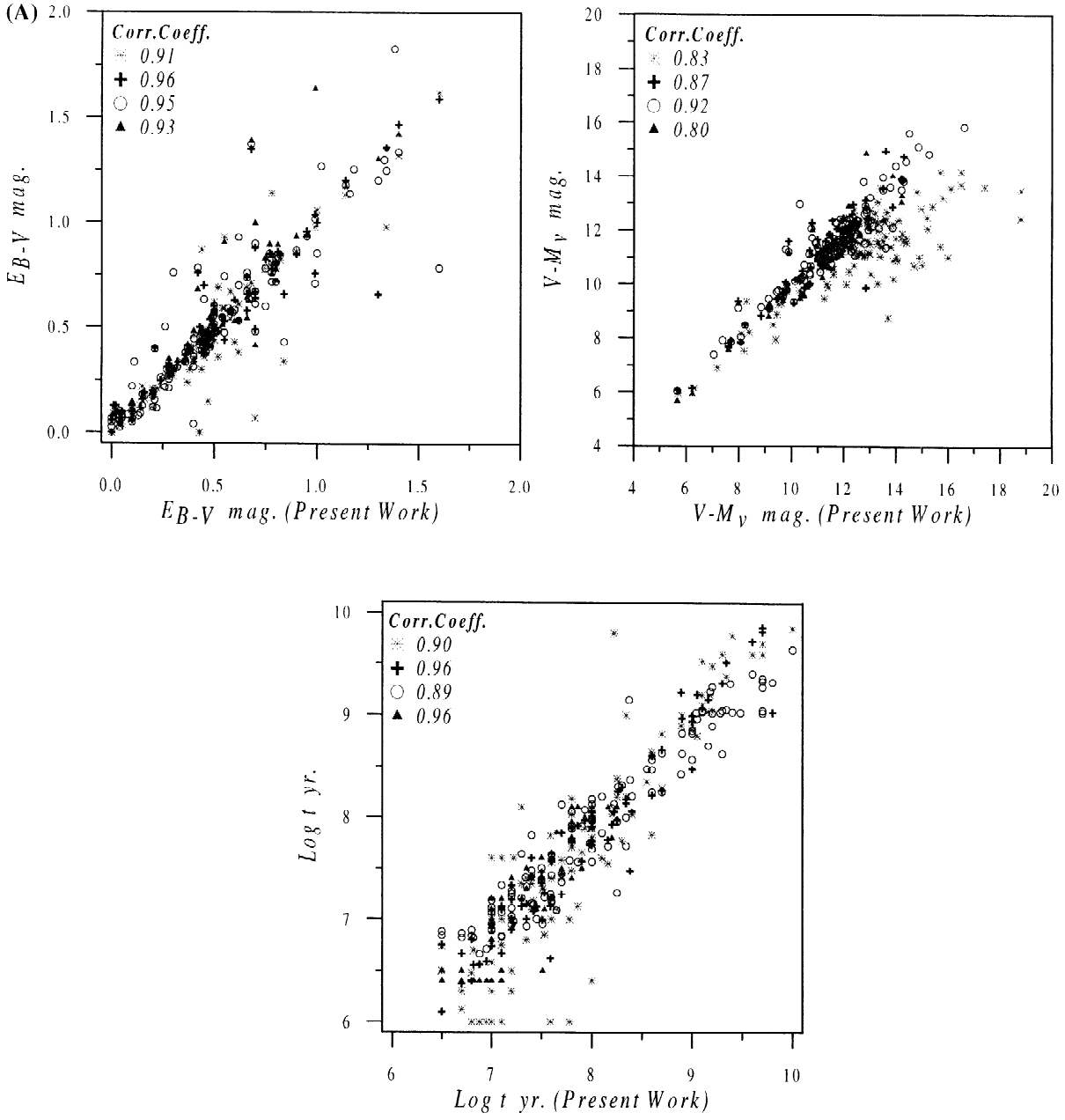

Fig. 1. (A) The comparsion of the main parameters, reddening, ages and distances, with the recent catalogs of Lyngå (1987): 102 clusters (asterisks); Loktin and Matkin (1994): 86 clusters (crosses); Loktin et al. (1997): 118 clusters (circles); and Dambis (1999) 60 clusters (triangles). (B) The comparsion of the present work with Twarog et al. (1997): 28 clusters (circles) for reddening and distance modulus and with Friel (1995): 39 clusters (triangles) for distance modulus.

galactocentric distances 8.0 and 9.5 kpc. We see that most clusters with small diameters ($D < 5$ pc) seem to be concentrated near the galactic plane, especially for $Rgc < 9.5$ kpc. Part of large-size clusters is old clusters, which are found far from the galactic center and also at larger distances from the galactic plane.

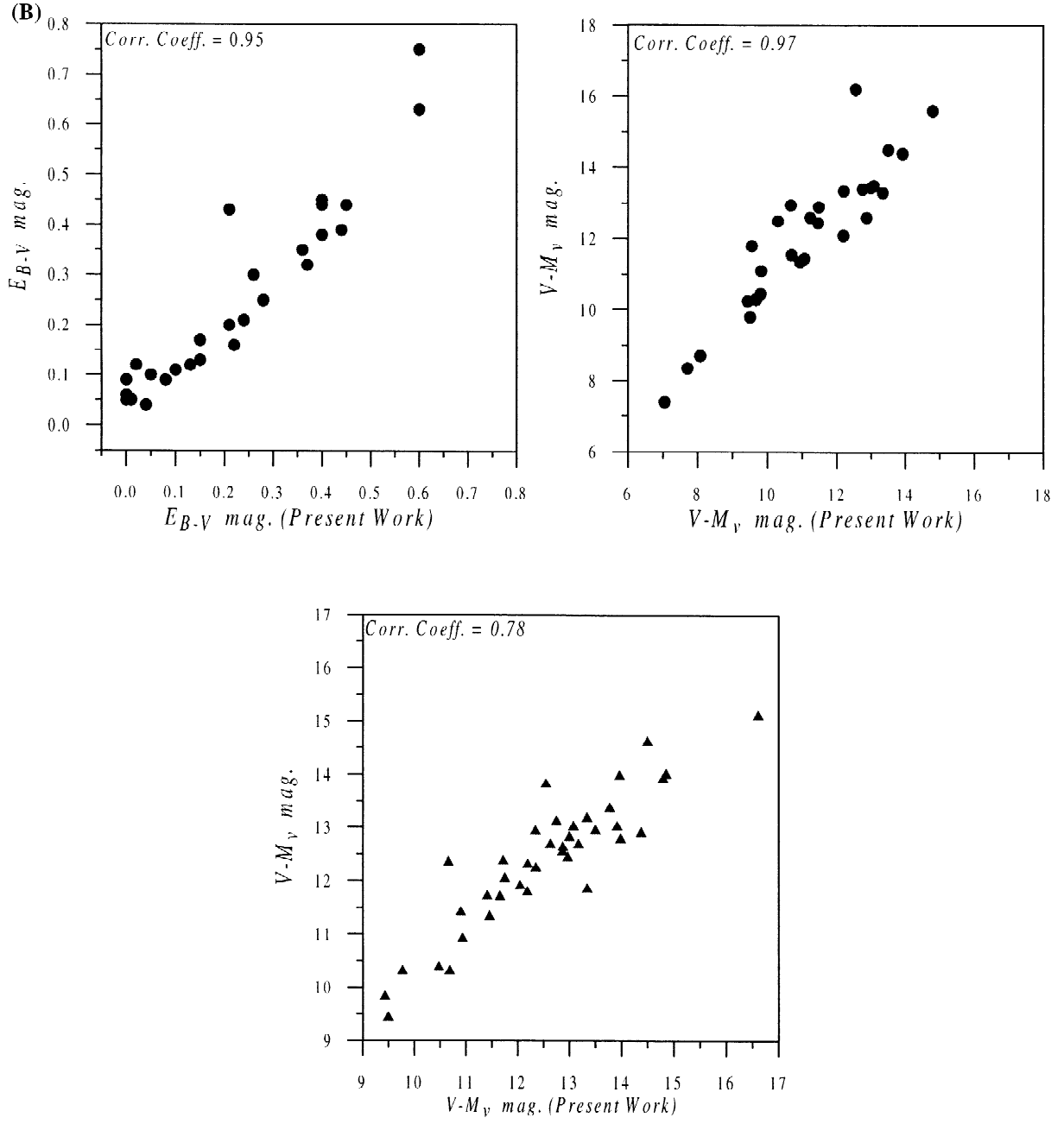

Fig. 1. (*continued*)

There are only a few clusters (young and located at $Rgc > 9.5$ kpc) larger than 15 pc; very young objects that belong to the galactic plane are loose and unbound objects of large diameter, hence quickly disrupted. We note here that our sample is missing most of the very young clusters present, e.g. in the Lyngå catalog.

The relation between the diameters and the galac-

Table 2
The numbers of shared clusters and the correlation coefficients for the comparisons of our main parameters with other recent catalogs

Catalog	Clusters no.	E_{B-V}	Log t	$V-M_v$
Lyngå, 1987	102	0.91	0.90	0.83
Loktin and Matkin, 1994	86	0.96	0.96	0.87
Friel, 1995	39	–	–	0.78
Loktin et al., 1997	118	0.93	0.96	0.79
Twarog et al., 1997	28	0.95	–	0.97
Dambis, 1999	60	0.95	0.89	0.92

tocentric distance has been examined in three ranges of ages: $t < 10^{8.0}$, $10^{8.0} < t < 10^{9.5}$, and $t > 10^{9.5}$ yr, see Fig. 8. We assume that errors in Rgc can be derived from uncertainties in the distance modulus, which increases with increasing distance from the Sun. Burki and Maeder (1976) found a correlation between those quantities only for the very young clusters, but we have found correlation's also for intermediate and old age clusters (correlation coefficients of 0.31, 0.60, and 0.71, respectively) as shown in Fig. 8.

3.4. Age–galactic height (Z)

The absolute values of the cluster's distances from the galactic plane, $|Z|$, has been plotted versus the clusters' ages as shown in Fig. 9. Most clusters with ages $t < 10^{8.8}$ yr are lying within $|Z| \approx 200$ pc, while older ones are lying also higher than such distances. It indicated that the thickness of the galactic disk has not changed on the time scale of about $10^{9.0}$ yr and the clusters can be formed everywhere inside this layer. On this consideration, the young cluster Be 93, which has age of $10^{8.0}$ yr and $|Z| < 800$ pc, is assumed to belong to the galactic warp as suggested by Saurer et al. (1994).

Age–Z relation has been examined in two different ranges of galactocentric radii, $Rgc < 9.5$ and $Rgc > 9.5$ kpc, respectively, as shown in Fig. 10. Lyngå and Palous (1987) have found that old clusters are much thicker distribution in the outer parts of the Galaxy than the inner parts. Also, in our study the thickness of the galactic disk at $Rgc > 9.5$ kpc is increasing for old clusters of $t > 10^{8.8}$ yr. The old clusters not only spend their time in the outer disk away from the disruptive effects of giant

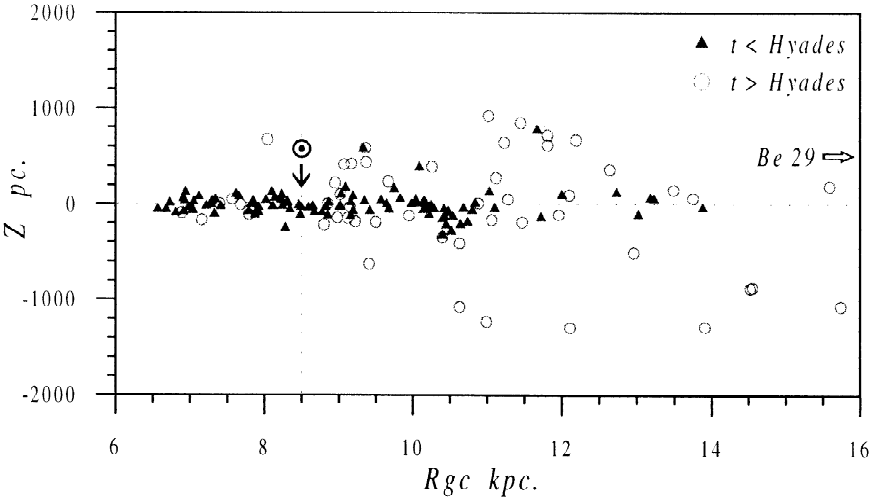

Fig. 2. The distribution of the clusters' sample according to their distances from the galactic center and the galactic plane for two ranges of clusters' age. The horizontal arrow refers to the cluster Be 29 while the vertical arrow refers to the position of the Sun.

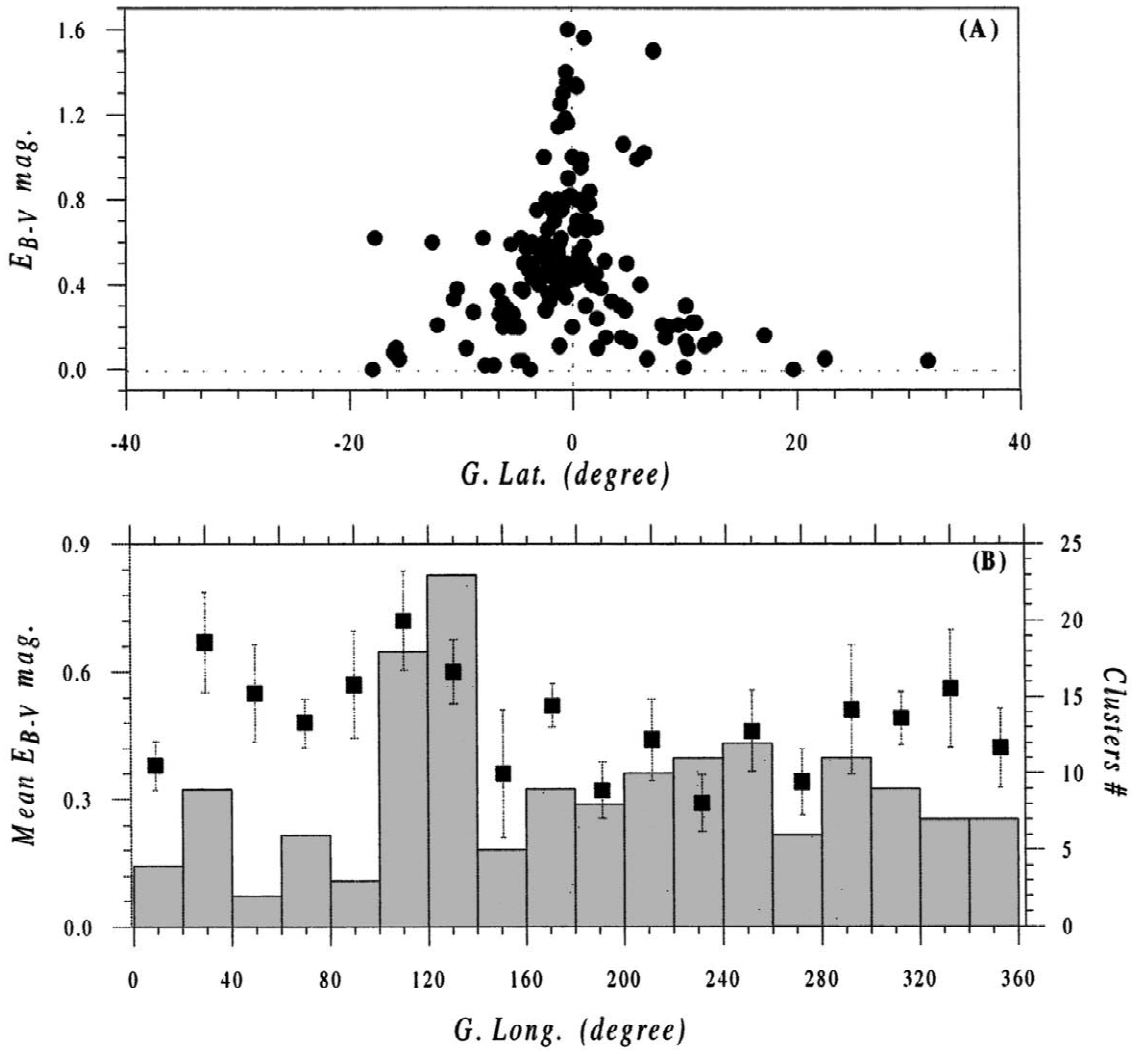

Fig. 3. (A) represents the reddening distribution with galactic latitudes. (B) represents the distribution of the mean reddening along the galactic longitudes with steps of 20 degrees (filled squares). The bars represent the standard errors of the mean reddening. The histogram represents the number of the clusters at each longitude bin.

molecular clouds, they spend their time at large distances from the galactic plane, further enhancing their survivability (Friel, 1995).

Zooming on the location of the sun with young clusters of $t < 10^{8.0}$ yr, we found that the maximum height above the galactic plane is less than 150 pc., while many clusters away from the sun vicinity are found to lie at distances of $Z \approx 300$ pc below the galactic plane. It is pointed to the largest and deepest depression in the vicinity of the sun (The Big Dent) that is about 1.5 kpc in diameter and reaching about 200 pc below the galactic plane (Cabrera-Cano et al., 1995).

3.5. Age–galactocentric radii (Rgc)

The previous studies implied that there is a lack of old clusters in the inner parts of the galactic disk,

Table 3
The mean reddening distribution along the galactic longitude bins

G. Long. bins	Clusters no.	$\langle E_{B-V}\rangle$	S.D.
0–20°	4	0.38	0.19
20–40°	9	0.67	0.39
40–60°	2	0.55	0.38
60–80°	6	0.48	0.19
80–100°	3	0.57	0.42
100–120°	18	0.72	0.39
120–140°	23	0.60	0.25
140–160°	5	0.36	0.50
160–180°	9	0.52	0.17
180–200°	8	0.32	0.22
200–220°	10	0.44	0.32
220–240°	11	0.29	0.22
240–260°	12	0.46	0.32
260–280°	6	0.34	0.26
280–300°	11	0.51	0.51
300–320°	9	0.49	0.21
320–340°	7	0.56	0.46
340–360°	7	0.42	0.31

and the anti-center clusters survive longer than such clusters. In the inner parts of the Galaxy they have never got the relaxation state in the fluctuating gravitational field of that parts (Lyngå, 1980; McClure et al., 1981; Vanden Bergh, 1985). This has been examined here, as shown in Fig. 11; note that clusters of $Rgc < 6.5$ kpc are completely missing in the present compilation, and this is in accord with what found, e.g. for old clusters by Friel (1995).

To show the effects of the completeness limit in our sample, we have binned clusters in galactocentric radius and age, as shown in Table 4. Of course, the parts near the solar vicinity ($8.0 < Rgc < 9.5$ kpc) are found to be more populated than other parts of the Galaxy, since the census of nearby objects is complete, while we miss more and more going farther. This is also more important for old and less luminous clusters than for young and high luminous ones (Janes et al., 1988), so the general trend we see implies that lifetime increases outwards in the Galaxy, where clusters live longer than those in the inner parts. We have also examined the clusters' positions in three different ranges of ages to localize the youngest clusters on the galactic disk: 25% of clusters in our sample have ages less than $10^{7.5}$ yr, and most of them are concentrated on the young outer arm of the Galaxy (Perseus arm).

3.6. Age–member richness

The relation between ages and clusters' member richness has been presented in Fig. 12, where the general trend can be expressed in the next equation:

$$\text{Log mem.} = 0.19\ \text{Log}\ t + 0.79$$

Although this relation has a weak correlation, it may confirm the fact that poor clusters tend to disrupt themselves easier than rich massive ones (Wielen, 1971). Open clusters may disrupt themselves by successive tidal encounters with interstellar clouds on a time scale of 10^8 to 10^9 yr. These disruption time scales depend strongly on both cluster mass and core radius. Apparently, the open clusters with ages of over a billion years have survived because of their larger than average mass, higher central concentration, and orbits that allow them to avoid the disruptive influence of the giant molecular clouds (Friel, 1995).

3.7. Age–diameter

Youngest clusters with large sizes are supposed to be some groups of OB stars associations and probably they are not bound systems (Lyngå, 1982; Janes et al., 1988). Mathieu (1986) confirms this concept from some direct radial velocity measurements of some well-known very young clusters, which are in fact some unbounded systems that will be dissolved in few million years. Massive clusters with small sizes will be dissolved due to encounters among their members, while those of very large sizes with the same mass will be unstable in the galactic tidal field, and they may take a very long time to have stability and relaxation (Theis, 2001). On this basis, the relation between ages and linear diameters has been examined for three different ranges of the distances from the galactic plane: $|Z| < 100$, $100 < |Z| < 500$ and $|Z| > 500$ pc, see Fig. 13. It is found that there is no strong correlation between diameters and ages, and clusters of large size are either young or belong to older population groups, which are large distances from the galactic plane. Small clusters with typical diameters less than 6 pc show a concentration to the galactic plane in the range of $|Z| < 100$ pc, (Wielen, 1971, 1975) but most large clusters have either intermediate or old ages. On the other hand, far away

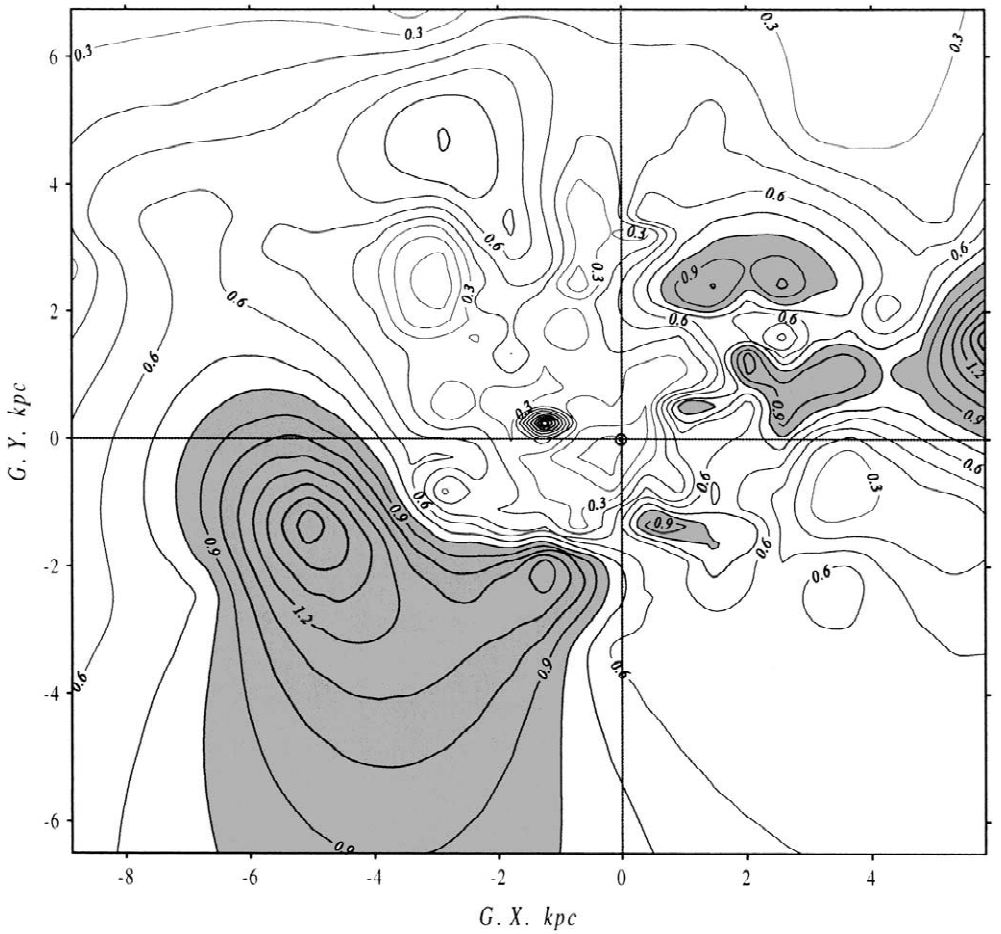

Fig. 4. Contour map of the reddening distribution on the galactic disk. Dark regions represent the higher values of reddening and vice versa. There are concentrations on three features pattern: Sagittarius, Carina and Perseus. The Sun is in the origin.

from the galactic plane $|Z| > 500$ pc, another group of old rich clusters can be seen with different distribution and intermediate sizes.

3.8. Luminosity function

A very important measured quantity for a cluster is the number of stars in a given range of color and visual magnitude. Many studies of luminosity functions and derived mass functions for old clusters show surprising flat distributions (Van den Bergh and Sher, 1960; Francic, 1989; Caputo et al., 1990; Aparicio et al., 1990; Montgomery et al., 1993). While luminosity functions for young open clusters continue to increase to fainter magnitudes and lower masses, in old clusters there is strong evidence for luminosity functions that either flatten, or reach a maximum, turn over, and decrease toward fainter magnitudes (Friel, 1995). Although the CCD system affected the magnitude limits of the clusters, and so many faint stares can be observed, sometimes and in many CCD studies, only the central part of the clusters are observed and so many stars are simply missed. However, to show what is called the net observed luminosity function of the clusters, the number of stars at intervals of one-magnitude for

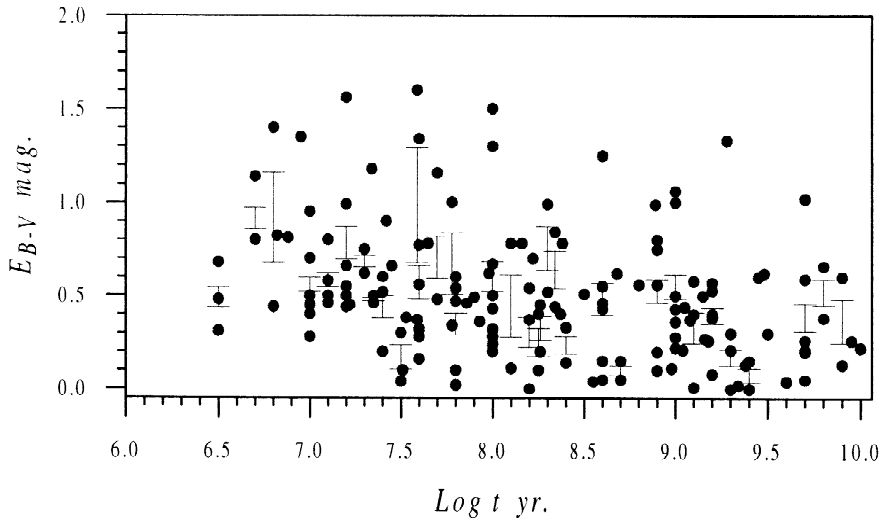

Fig. 5. The relation between the clusters' ages and reddening. The bars represent the mean standard errors at the average points.

member and field stars have been constructed. One-magnitude intervals have been selected to include reasonable number of stars per magnitude bin for the best possible statistical variation of the luminosity and mass functions, whereas the property that makes the clusters different from the field stars is the mass (Twarog et al., 1997). The luminosity of each member has been obtained from its visual magnitude according to the relation:

$$\mathrm{Log}\, L/\mathrm{L}_{\odot} = 0.4 * (4.79 - M_{\mathrm{v}})$$

where the visual absolute magnitude (M_v) of a member star equals its visual magnitude subtracted

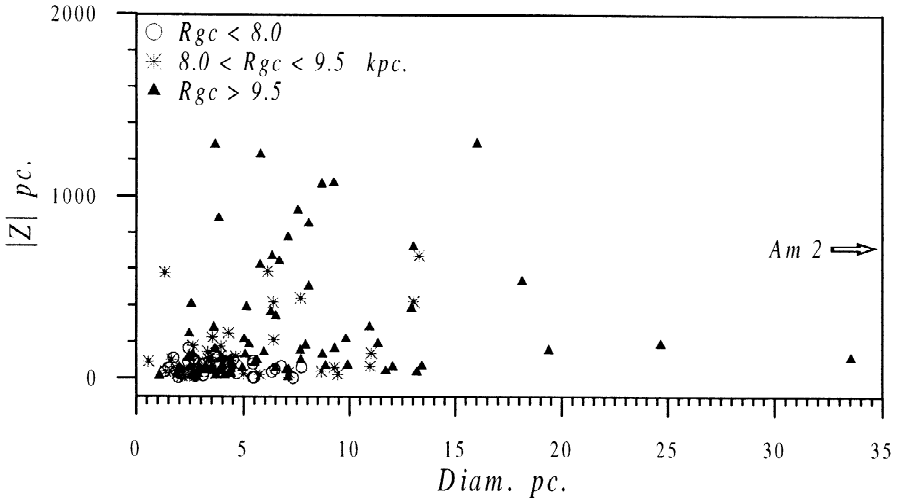

Fig. 6. The relation between the linear diameters and the absolute distances from the galactic plane—|Z|—in three different ranges of the galactocentric radii.

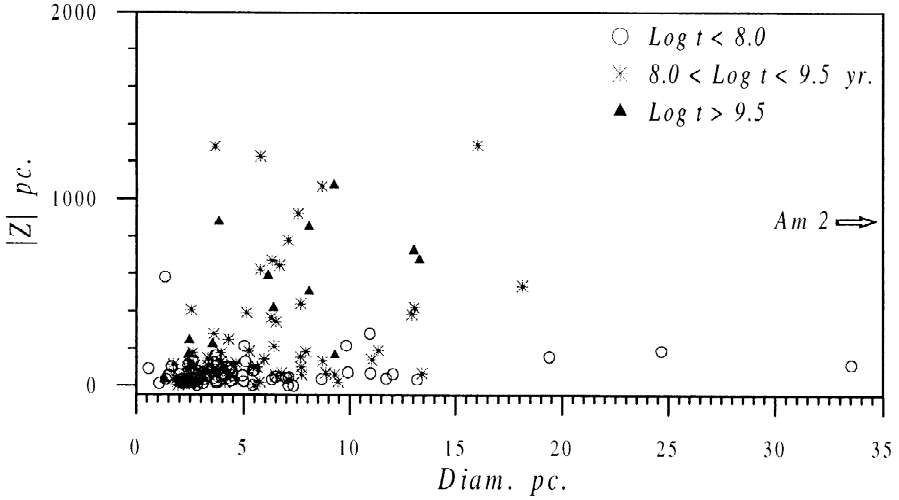

Fig. 7. The relation between the linear diameters and the absolute distances from the galactic plane—$|Z|$—in three different range of ages.

from the distance modulus of the cluster it belongs to. So according the relation between the cluster luminosity and the total visual magnitude, the luminosity function of a cluster can be obtained by summing up the visual luminosity of every member it has. Related to the peak values of the member and field stars of each cluster, the visual luminosity function of the entire sample can be obtained as shown in Fig. 14.

The relation between ages and the visual luminosity of our sample has been studied and plotted in Fig. 15. It can be represented as:

$$\mathrm{Log}\, t = 0.26\, M_{\mathrm{v}} + 9.30$$

3.9. Mass function

Salpeter (1955) defined the initial mass function of a cluster as:

$$\Phi(M/\mathrm{M}_{\odot}) = \Theta * (M/\mathrm{M}_{\odot})^{\eta}$$

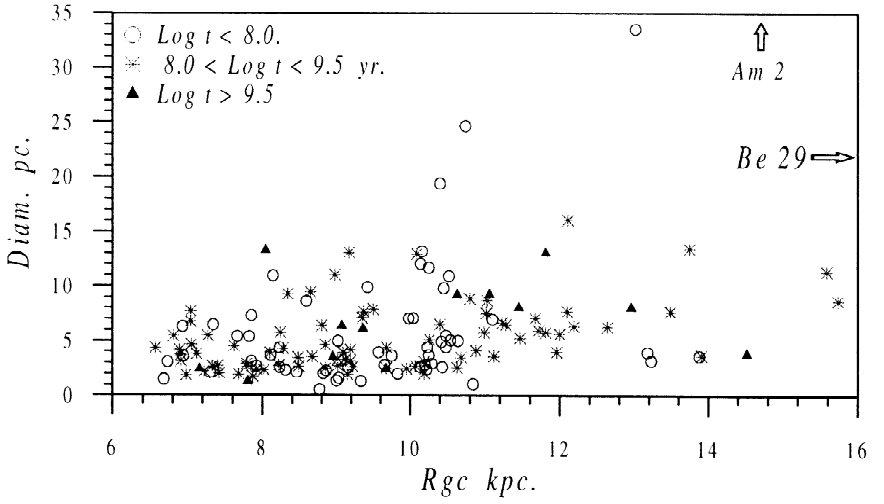

Fig. 8. The relation between the galactocentric radii, *Rgc*, and linear diameters in three different ranges of ages.

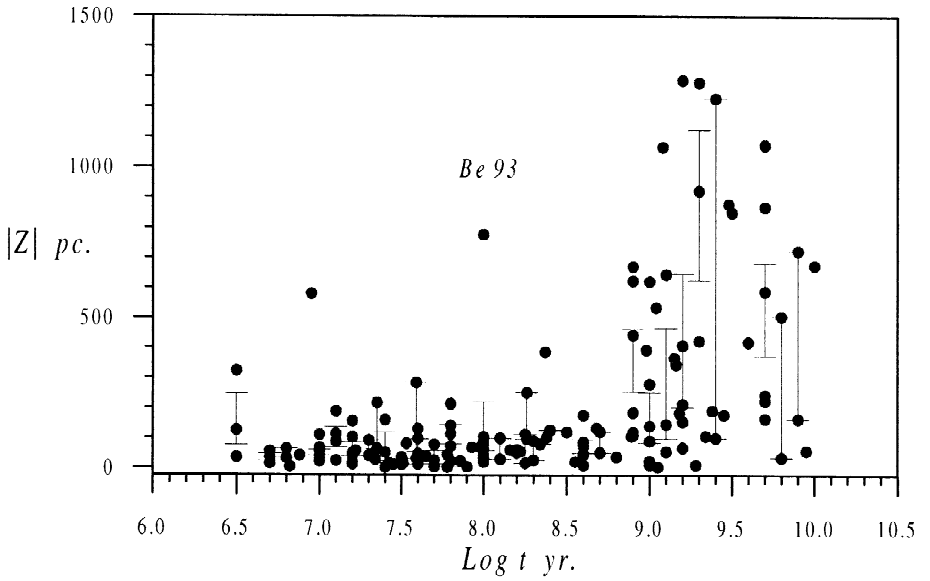

Fig. 9. The relation between the clusters' ages and the absolute distances from the galactic plane $|Z|$. The bars represent the mean standard errors at the average points.

He found $\Theta = 0.03$ and $\eta = -1.35$. The mass function of clusters and its evolution with time have been studied by many authors (see e.g. the review by Scalo (1998), or the work of De Marchi and Paresce (2001), Prisinzano et al. (2001) and Muench et al. (2002)). In the present study, the mass function of every cluster has been estimated using the theoretical evolutionary tracks and their isochrones of Vanden Bergh (1985). The masses of the clusters' members have been estimated from one of the polynomial equations that have been developed from the isochrones data of different ages at the metallicity factor $z = 0.0169$. The mass function histograms have been constructed by dividing the mass scale into suitable

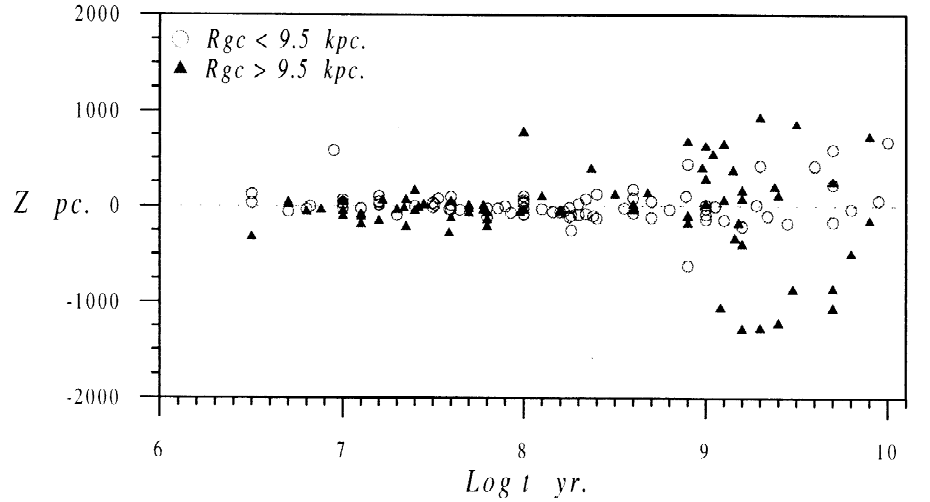

Fig. 10. The relation between ages and distances from the galactic plane in two ranges of galactocentric radii.

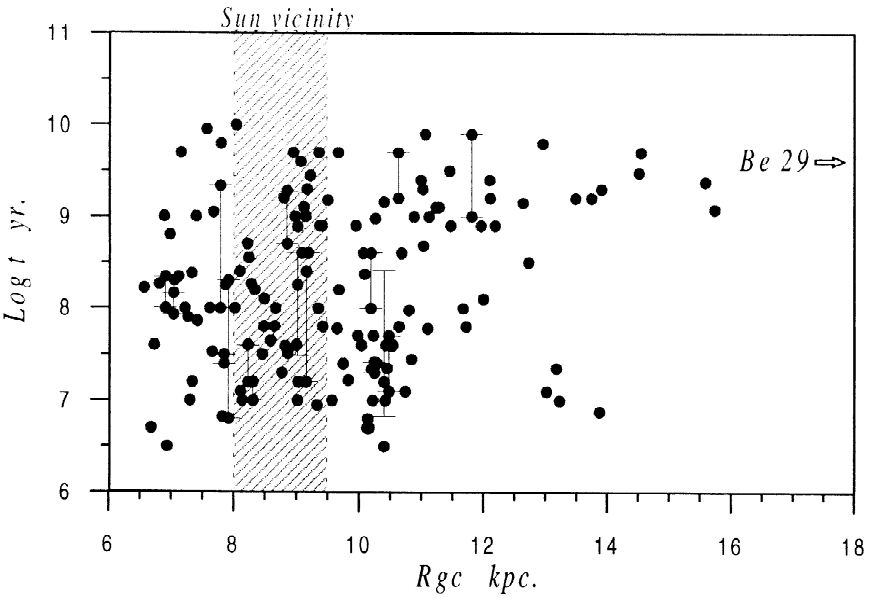

Fig. 11. The relation between the galactocentric radii and ages. The bars represent the mean standard errors at the average points.

bins and counting the number of stars at each bin. Applying the power law fitting on the mass function histograms, Θ and η are found to be different from what we have obtained from the classical observations, which may be related to the large number of faint stars that detected by using CCD systems.

On this concept, the masses of the clusters have been estimated by summing up the stars in each bin weighted by the mean mass of that bin. A histogram of the cluster masses for the whole set of our sample has been plotted in Fig. 16; the beak value of the mass function has been found to lie at 794 $M_{\odot}$, which is found to be more than what we expected using the classical observations. A running average polynomial fitting of second order has been applied to the histogram and the beak value of the mass function is found to be lie at 400 $M_{\odot}$, which is higher than (360 $M_{\odot}$) that estimated by Reddish (1978). In addition, the index of the power law is found to be -2.11, which is higher than (-2.20) that obtained by Reddish (1978) also. According the number of members we have at the mass peak of every individual cluster, the mass function of our entire sample has been constructed as shown in Fig. 17.

Table 4
Number of clusters in different ranges of Rgc and age

Rgc bins	Log *t*				Total
	6–7	*7–8*	*8–9*	*9–10*	
<8.0	6	12	12	5	35
8.0–9.5	1	21	17	9	48
9.5–11.0	4	24	9	7	44
11.0–12.5	–	2	6	10	18
12.5–14.0	1	3	1	5	10
>14.0	–	–	–	5	5

3.10. Mass–diameter and member richness

Although Wielen (1971) has suggested that any cluster with mass of 500 $M_{\odot}$ have optimum survivability with linear diameter of $2 \leq D \leq 4$ pc, Janes et al. (1988) supposed that the correlation between clusters' masses and diameters is very weak. However, in the present work, this relation has been examined for three different ranges of age: $t < 10^{8.0}$, $10^{8.0} < t < 10^{9.5}$, and $t > 10^{9.5}$ yr, as shown in Fig. 18, and good correlation between masses and diame-

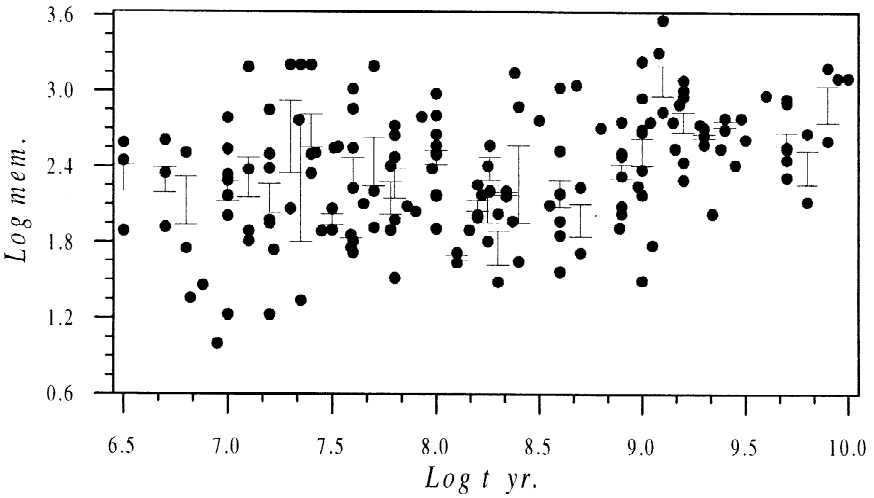

Fig. 12. The relation between the clusters' ages and member richness. The bars represent the mean standard errors at the average points.

ters have been found with correlation coefficients of 0.26, 0.35 and 0.71, respectively. For old clusters, the correlation is found more pronounced than those of the young and intermediate ones, which implied that old massive clusters have more stable diameters than younger ones are. Some open clusters, particularly those older than $10^{9.0}$ yr, are significantly more massive than has been commonly thought (Friel, 1995).

From our sample, three ranges of masses could be obtained as follows:

	Cluster No.	Mean Mass
$M < 500$ M$_\odot$	92	233
$500 < M < 1000$ M$_\odot$	40	718
$M > 1000$ M$_\odot$	28	1708

A correlation coefficient of 0.87 has been found between the cluster's mass and the members' richness as shown in Fig. 19, where

Log mass = 0.77 Log mem. + 0.75

It is interesting to note that most massive clusters are

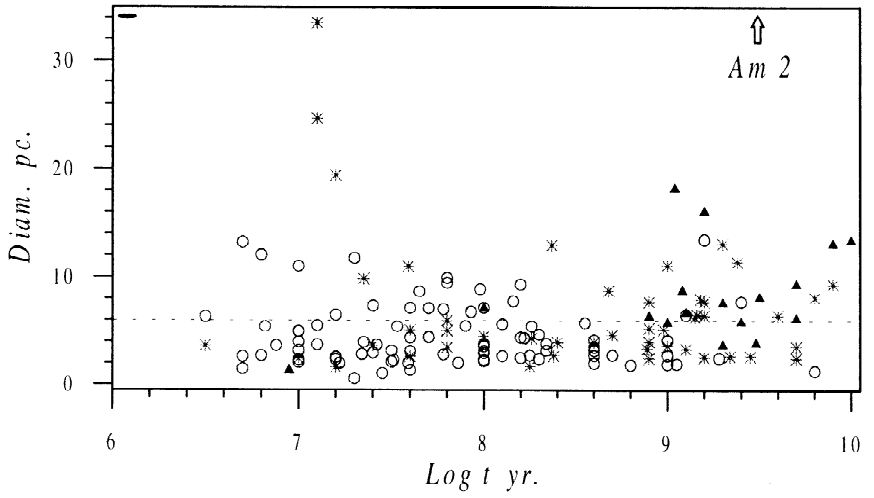

Fig. 13. The relation between the clusters' ages and linear diameters in three different ranges of distances from the galactic plane.

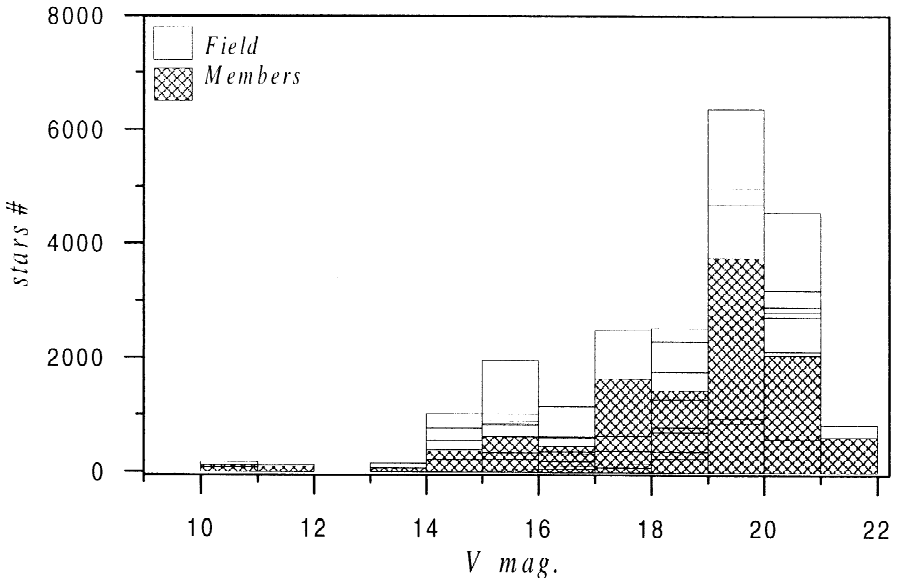

Fig. 14. Luminosity function for the entire sample rested on the field and members' peak of each cluster.

concentrated in the outer parts of the galactic disk, and vice versa.

3.11. Galactic spiral arms

Several optical and radio studies have been carried out in the last 40 years in order to show the shape of the spiral arms of the Galaxy. So, the positions of the clusters on the galactic plane have been used to trace the galactic spiral arms. Centered on the sun (at $X = 0$ and $Y = 0$) the distribution of the clusters on the galactic plane has been plotted for three ranges of

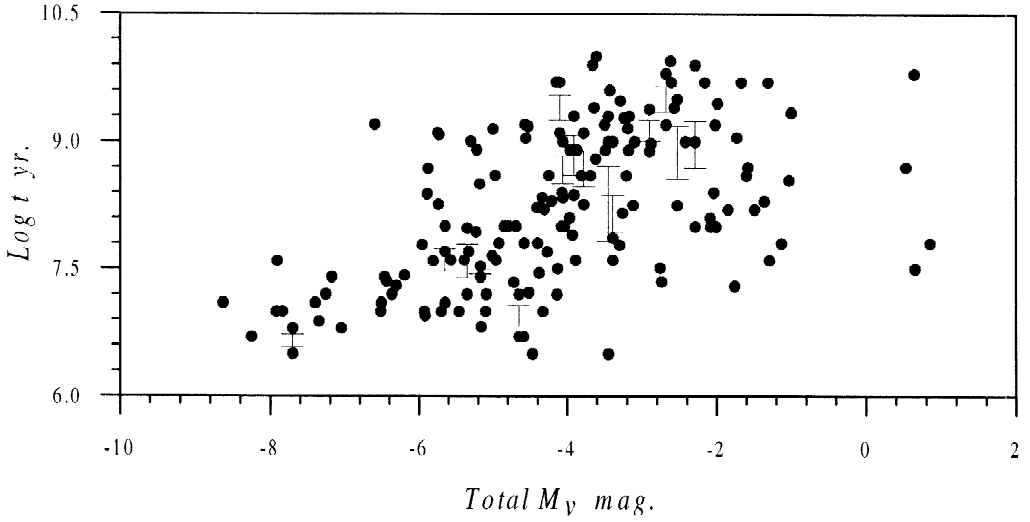

Fig. 15. The relation between the clusters' total visual magnitudes and ages. The bars represent the mean standard errors at the average points.

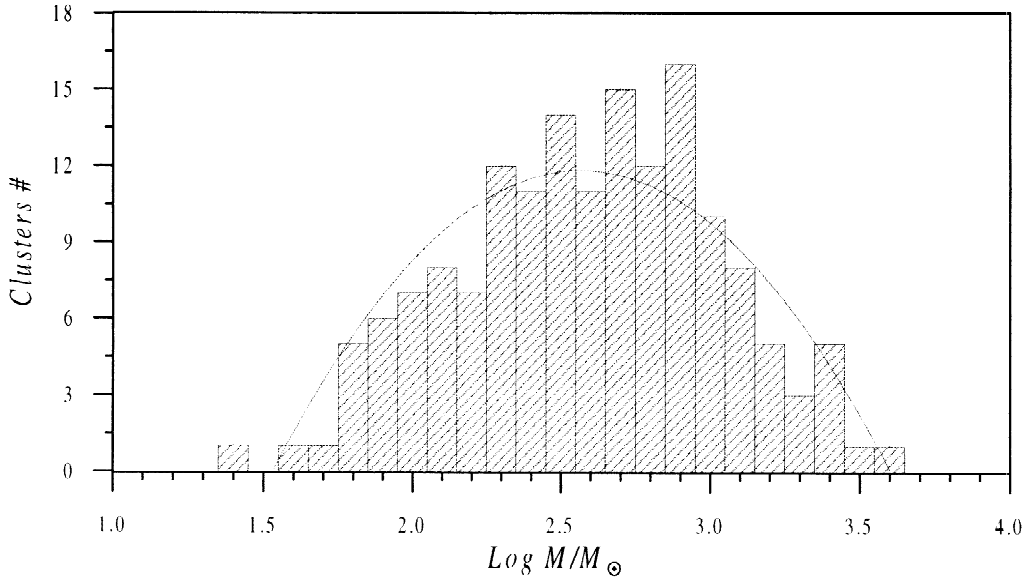

Fig. 16. Histogram of the clusters' masses for the whole set of our sample.

ages: $t < 10^{8.0}$, $10^{8.0} < t < 10^{9.5}$, and $t > 10^{9.5}$ yr, as shown in Fig. 20. Old cluster distribution doesn't show any structure, while within a radius of 4 kpc from the sun (cf. Janes et al., 1988); the distribution of the intermediate and young clusters define three concentration features which are related to the spiral structure of the Galaxy: Perseus, Carina and Sagittarius. It is assumed that there are more than three arms for the Galaxy but because of the patchy cloud and absorption effects we are unable to detect them

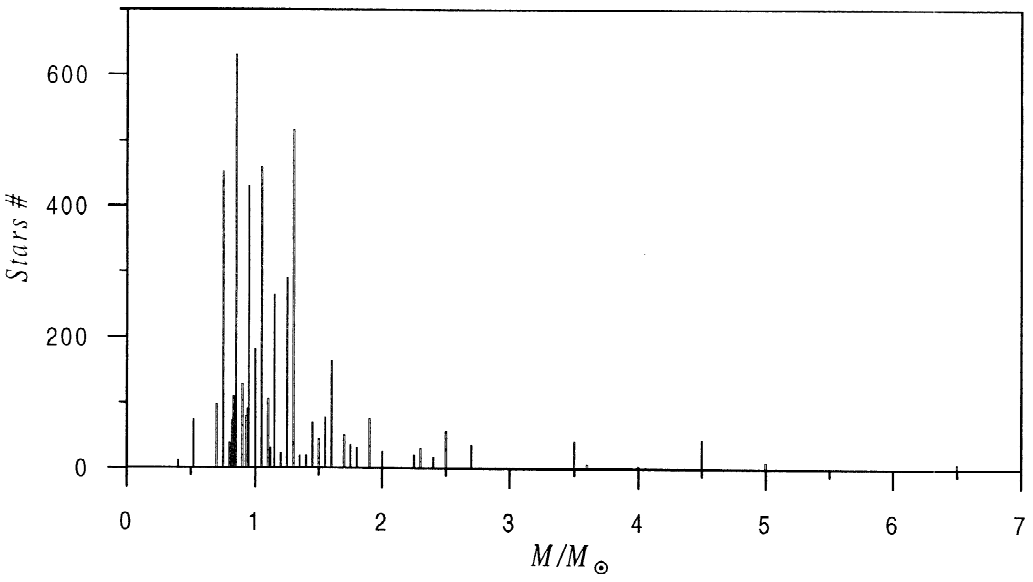

Fig. 17. Mass function for the entire sample rested on the masses' peaks of each cluster.

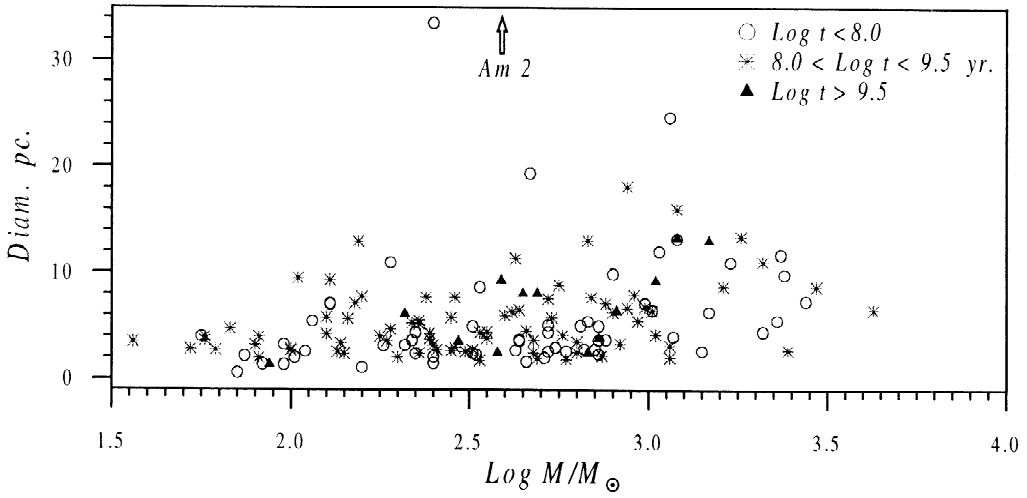

Fig. 18. The relation between the clusters' masses and linear diameters in three different age ranges.

all. Also, a sample of 160 open clusters is insufficient to detect the rest arms on the galactic disk.

3.12. Galactic warp

The effect of the galactic warp may be declared from the distribution of the open clusters of our sample using the galactic coordinates X and Y versus the height Z within ± 2 kpc from the galactic plane as shown in Fig. 21. The directions of X and Y defined to be positive in the direction of galactic rotation and radially outward respectively (Janes et al., 1988). No strong indication to the warp existence has been found on the galactic disk. This may refer to the leak of the clusters' number,being large distances from the sun vicinity.

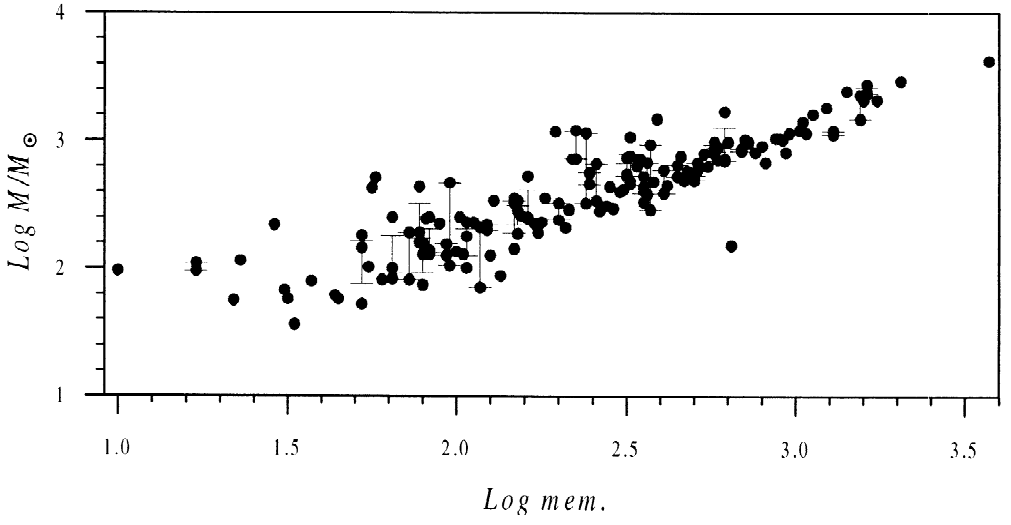

Fig. 19. The relation between the clusters' member richness and masses. The bars represent the mean standard errors at the average points.

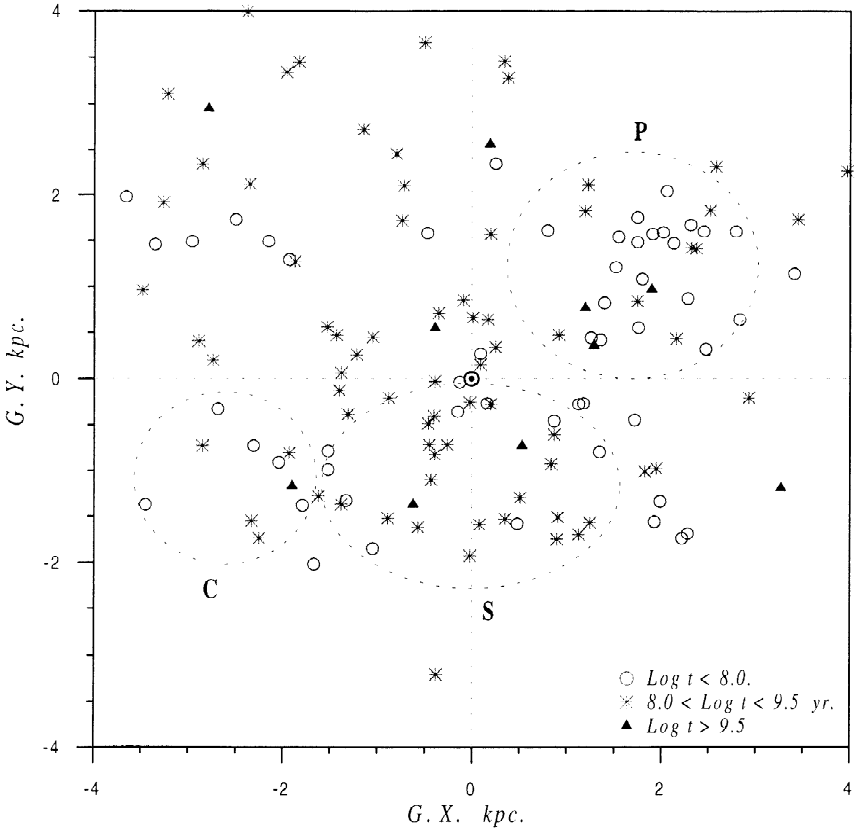

Fig. 20. The distribution of the clusters' sample in the galactic plane with three different ranges of ages. The three dashed circles refer to the three famous arms of the Galaxy: Sagittarius (S), Carina (C), and Perseus (P).

4. Conclusions

It is obvious that CCD systems affected the magnitude limit of the clusters, which makes many faint stars to be detected on the lower parts of the color magnitude diagrams. The fitting of the color-magnitude diagrams with standard age main sequence becomes much easier with CCD observations. This, of course, has contributed to the evaluation of the cluster parameters: distances (diameters), ages, reddening, etc. The most parameter that is affected by CCD-system is the membership richness that the luminosity function and consequently the mass function too. In this paper we studied the behavior of the clusters' properties on the galactic desk with each other depending mainly on the homogeneous catalogue of Tadross (2001). To declare the evolution of the clusters' properties with age, the mean statistical values of these parameters at age steps of $10^{0.5}$ yr. are estimated and tabulated in Table 5. This kind of study may give more accurate results if we have a large homogeneous catalogue of CCD data (i.e. more than 160 open clusters).

Acknowledgements

Many thanks are presented to Professor Roland Buser (Bern University, Switzerland) and Professor Wilhelm Seggewiss (Hoher List University Observatory, Bonn, Germany) for their valuable remarks and critically reading the original version of this work. Special thanks go to Professor Emilio J. Alfaro

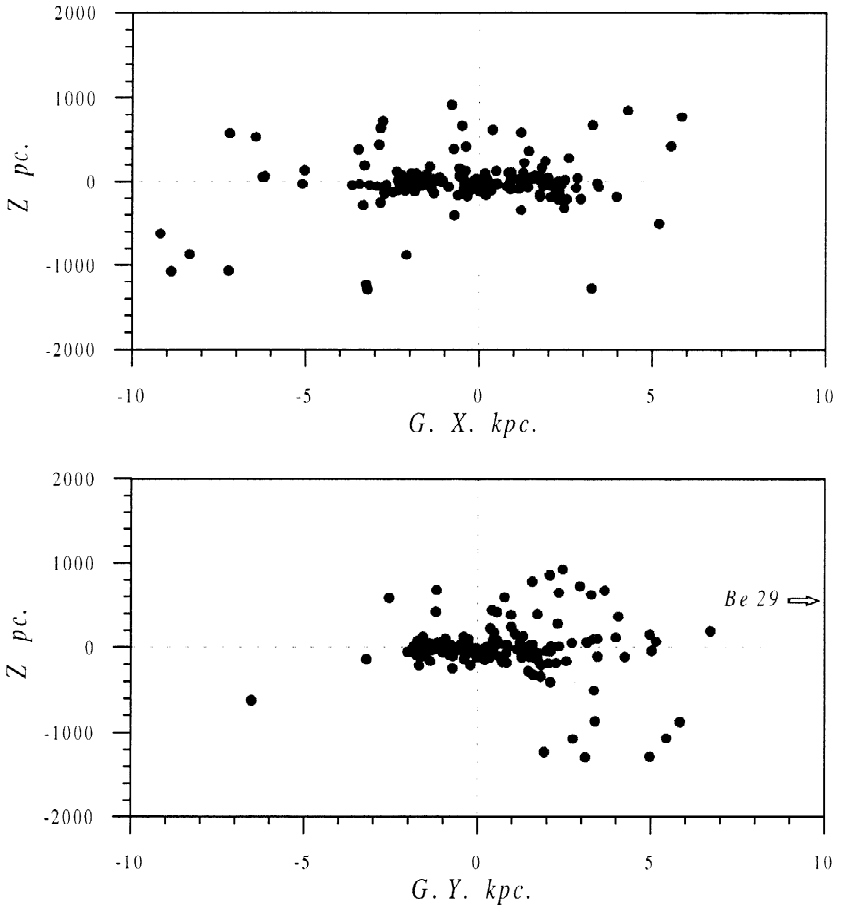

Fig. 21. The distribution of the clusters' sample according to their galactic coordinates X and Y with distances from the galactic plane Z. The sun's position is at $X = Y = 0$.

Table 5
Statistical correlation of the mean parameters with age bins

Parameter	Log t					
	<7.5	7.5–8.0	8.0–8.5	8.5–9.0	9.0–9.5	>9.5
M_v	−5.8	−4.2	−3.7	−3.7	−3.4	−2.6
E_{B-V}	0.68	0.52	0.51	0.45	0.39	0.35
Z	81	67	112	177	386	470
Rgc	9.6	9.3	8.4	9.9	11.5	10.0
L. Diam.	6.1	5.2	4.5	4.3	6.6	11.5
Richness	390	340	220	370	670	670
Mass	815	505	370	490	830	665
Mass/mem.	3.2	1.9	1.9	1.7	1.2	1.0

(Institute of Astrophysics, Andalucia, Spain) for his valuable discussions and suggestions about this work.

References

Aparicio, A. et al., 1990. A&A 240, 262.

Burki, G., 1975. A&A 43, 37.
Burki, G., Maeder, A., 1976. A&A 51, 247.
Cabrera-Cano, J. et al., 1995. ApJ 448, 149.
Caputo, F. et al., 1990. AJ 99, 261.
Dambis, A.K., 1999. AstL 25, 7.
Dutra, C., Bica, E., 2000. A&A 359, 347.
De Marchi, G., Paresce, F., 2001. Astronomische Gesellschaft Abstract Series, 18, the Annual Scientific Meeting JENAM 2001, abstract #MS 05 51.
Fernie, J., 1963. AJ 68, 780.
Friel, E.D., 1995. ARA&A 33, 381.
Francic, Sp., 1989. AJ 98, 888.
Janes, K., Tilley, C., Lyngå, G., 1988. AJ 95, 771.
Kholopov, P.N., 1980a. Soviet Astronomy 24, 7.
Kholopov, P.N., 1980b. Astronomicheskii Zhurnal 57, 12.
Loktin, A., Matkin, N., 1994. A&A Trans. 4, 153.
Loktin, A.V. et al., 1997. BaltA 6, 316.
Lyngå, G., 1987. Catalog of open cluster data, 5th ed., stellar data centers, Observatoire de Strasbourg, France.
Lyngå G., 1980. IAU symposium, 85, 13, Hesser J.E. (Ed.), Reidel, Dordrecht.
Lyngå, G., 1982. A&A 109, 213.
Lyngå, G., Palous, J., 1987. A&A 188, 35.
Maeder, A., Meynet, G., 1991. A&AS 89, 451.
Majewski, S. et al., 2001. American Astronomical Society Meeting 198, #62.13.
Malysheva, L., 1997. AstL 23, 585.
Mathieu, R., 1986. Highlight Astron. 7, 481.
McClure, R. et al., 1981. ApJ 243, 841.
Montgomery, K.A. et al., 1993. AJ 106, 181.
Muench, A. et al., 2002. ApJ 573, 366.
Perryman, M. et al., 2001. A&A 369, 339.
Prisinzano, L. et al., 2001. A&A 369, 851.
Reddish, V., 1978. Stellar Formation. Pergamon Press, Oxford.
Salpeter, E., 1955. ApJ 121, 161.
Saurer, W. et al., 1994. AJ 107, 2101.
Scalo, J., 1998. ASP Conference Series, 142, The Stellar Initial Mass Function; 38th Herstmonceux Conference, 201.
Tadross, A.L., 2001. NewA 6, 293.
Theis, Ch., 2001. Astronomische Gesellschaft Abstract Series, 18, the Annual Scientific Meeting JENAM 2001, abstract # MS 05 47.
Twarog, B. et al., 1997. AJ 114, 2556.
Vanden Bergh, D., 1985. Astrophys. Suppl. 58, 711.
Van den Bergh, S., Sher, D., 1960. Publ. David Dunlap Obs. 2, #7.
Wielen, R., 1971. A&A 13, 309.
Wielen R., 1975., IAU symposium 69, 119, Hayli, A. (Ed.), Reidel, Dordrecht.
Worthey, G., 2001. American Astronomical Society Meeting 198, #62.12.